Accurate measurements of the thermal diffusivity of thin filaments by lock-in thermography

Agustín Salazar,[1,a)] Arantza Mendioroz,[1] Raquel Fuente,[1] and Ricardo Celorrio[2]
[1]*Departamento de Física Aplicada I, Escuela Técnica Superior de Ingeniería, Universidad del País Vasco, Alameda Urquijo s/n, 48013 Bilbao, Spain*
[2]*Departamento de Matemática Aplicada, EUITIZ, Universidad de Zaragoza, Campus Río Ebro, Edificio Torres Quevedo, 50018 Zaragoza, Spain*

(Received 17 December 2009; accepted 8 January 2010; published online 18 February 2010)

In lock-in (modulated) thermography the lateral thermal diffusivity can be obtained from the slope of the linear relation between the phase of the surface temperature and the distance to the heating spot. However, this slope is greatly affected by heat losses, leading to an overestimation of the thermal diffusivity, especially for thin samples of poor thermal conducting materials. In this paper, we present a complete theoretical model to calculate the surface temperature of filaments heated by a focused and modulated laser beam. All heat losses have been included: conduction to the gas, convection, and radiation. Monofilaments and coated wires have been studied. Conduction to the gas has been identified as the most disturbing effect preventing from the direct use of the slope method to measure the thermal diffusivity. As a result, by keeping the sample in vacuum a slope method combining amplitude and phase can be used to obtain the accurate diffusivity value. Measurements performed in a wide variety of filaments confirm the validity of the conclusion. On the other hand, in the case of coated wires, the slope method gives an effective thermal diffusivity, which verifies the in-parallel thermal resistor model. As an application, the slope method has been used to retrieve the thermal conductivity of thin tubes by filling them with a liquid of known thermal properties. © *2010 American Institute of Physics*. [doi:10.1063/1.3309328]

I. INTRODUCTION

Lock-in thermography consists in illuminating the sample by an intensity modulated light beam and detecting the oscillating component of the temperature rise by means of an infrared (IR) video camera connected to a lock-in module.[1] Lock-in thermography has been broadly used to measure the thermal diffusivity (D) of a wide variety of materials. In a typical setup, a modulated laser beam is focused onto the sample surface while the IR camera records the surface temperature. Under ideal conditions (absence of heat losses and absence of diffraction effects), for a given modulation frequency (f), both the natural logarithm of the amplitude of the oscillating temperature, $Ln(\tilde{T})$,[2] and its phase (ψ) depend linearly on the radial distance to the heating spot, with the same slope given by $m=-\sqrt{\pi f/D}$, from which the thermal diffusivity can be obtained (the so-called slope method).[3,4] This simple method has been successfully applied to good thermal conductors. However, it fails when dealing with poor thermal conductors (e.g., polymers, composites, biological samples, etc.). Actually, at medium and high frequencies the diffraction of the IR radiation crossing the lens of the camera increases the slope m leading to an overestimation of the thermal diffusivity.[5] On the other hand, at low frequencies the effect of heat losses increases the slope m producing also an overestimation of D. This effect is especially disturbing for thin films or thin filaments. For instance, the thermal diffusivity of a 25 μm thick polyimide film was found to be 1.12 mm^2/s, which is very much higher than the typical values of polymers (0.1–0.2 mm^2/s).[6] In the same way, thermal diffusivity values of human hair in the range 2–4 mm^2/s, an anomalously high value for a biological sample, have been reported.[7]

Recently, a complete model has been developed to include the effect of heat losses in the surface temperature of thin plates.[8,9] According to this model, heat conduction to the surrounding gas has been identified as the main mechanism responsible for the inaccuracy of the slope method. It has been demonstrated that by keeping the sample in vacuum while using low frequencies to avoid diffraction, the slope method combining amplitude and phase allows to retrieve the accurate value of the thermal diffusivity of thin plates.

In this paper, we present an extension of those previous works to filaments. First, we develop the theoretical model proposed by Barkyoumb and Land[10] to calculate the surface temperature of filaments by including all heat losses (conduction to the gas, convection, and radiation). Monofilaments as well as coated wires have been studied. As in the case of thin plates, conduction to the gas has been identified as the most disturbing effect preventing from the direct use of the slope method to measure the thermal diffusivity. Consequently, by keeping the sample in vacuum the slope method can be used to obtain the accurate D value. Measurements performed in a wide variety of filaments confirm the validity of the conclusion. On the other hand, in the case of coated wires, the effective thermal diffusivity given by the slope method verifies the in-parallel thermal resistor model. Accordingly, the slope method has been used to retrieve the

[a)]Author to whom correspondence should be addressed. Electronic mail: agustin.salazar@ehu.es.

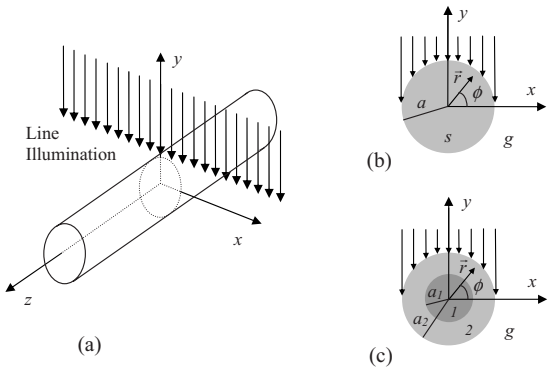

FIG. 1. (a) Diagram of a filament illuminated by a line laser beam. (a) Cross section of a monofilament and (b) of a coated wire.

thermal conductivity of thin tubes by filling them with a liquid of known thermal properties, as water.

II. THEORY

In this section we calculate the oscillating temperature of an opaque filament illuminated by a laser beam modulated at a frequency f ($\omega=2\pi f$). The laser beam is focused by a cylindrical lens to obtain a line shape with a Gaussian profile of radius b (at $1/e^2$), perpendicular to the filament. The power linear density of the laser is P_o (W/m). The geometry of the problem is shown in Fig. 1(a). Heat losses by conduction and convection to the surrounding gas and by radiation are taken into account. The temperature is obtained by solving the heat diffusion equation in the filament and in the surrounding gas which in cylindrical coordinates writes

$$\frac{\partial^2 T_i}{\partial r^2}+\frac{1}{r}\frac{\partial T_i}{\partial r}+\frac{1}{r^2}\frac{\partial^2 T_i}{\partial \phi^2}+\frac{\partial^2 T_i}{\partial z^2}-\frac{1}{D_i}\frac{\partial T_i}{\partial t}=0, \tag{1}$$

where D is the thermal diffusivity and $i=g$ (gas),s (sample). Due to the modulated excitation the temperature can be written as $T(r,z,\phi,t)=\tilde{T}(r,z,\phi)e^{i\omega t}$. Accordingly, Eq. (1) reduces to

$$\frac{\partial^2 \tilde{T}_i}{\partial r^2}+\frac{1}{r}\frac{\partial \tilde{T}_i}{\partial r}+\frac{1}{r^2}\frac{\partial^2 \tilde{T}_i}{\partial \phi^2}+\frac{\partial^2 \tilde{T}_i}{\partial z^2}-q_i^2\tilde{T}_i=0, \tag{2}$$

where $q=\sqrt{i\omega/D}$ is the thermal wave vector. This equation can be solved by using the Fourier transform

$$\tilde{T}(r,z,\phi)=\int_{-\infty}^{\infty}e^{i\lambda z}t(r,\lambda,\phi)d\lambda. \tag{3}$$

Likewise, Eq. (2) can be expressed in terms of its Fourier transform

$$\frac{\partial^2 t_i}{\partial r^2}+\frac{1}{r}\frac{\partial t_i}{\partial r}+\frac{1}{r^2}\frac{\partial^2 t_i}{\partial \phi^2}-\delta_i^2 t_i=0, \tag{4}$$

where $\delta_i^2=q_i^2+\lambda^2$. By using the separation of variables method, i.e., $t(r,\lambda,\phi)=R(r,\lambda)\Phi(\phi)$, Eq. (4) reduces to the following two equations

$$r^2\frac{d^2R_i}{dr^2}+r\frac{dR_i}{dr}-(\delta_i^2r^2+n^2)R=0, \tag{5a}$$

$$\frac{d^2\Phi_i}{d\phi^2}+n^2\Phi_i=0. \tag{5b}$$

Equation (5a) is the modified Bessel's differential equation, whose solutions are the modified Bessel functions:[11] $I_n(\delta_i r)$ and $K_n(\delta_i r)$. On the other hand, the solution of Eq. (5b) is the exponential function $e^{in\phi}$, with $n\in Z$.

A. Monofilament

In the case of a homogenous filament of radius a [see Fig. 1(b)], the oscillating temperature in the filament and in the surrounding gas can be written as

$$\tilde{T}_g(r,z,\phi)=\int_{-\infty}^{\infty}e^{i\lambda z}\left[\sum_{n=-\infty}^{\infty}A_nK_n(\delta_g r)e^{in\phi}\right]d\lambda, \tag{6a}$$

$$\tilde{T}_s(r,z,\phi)=\int_{-\infty}^{\infty}e^{i\lambda z}\left[\sum_{n=-\infty}^{\infty}B_nI_n(\delta_s r)e^{in\phi}\right]d\lambda. \tag{6b}$$

Note that in $\tilde{T}_g$ only K_n appears since $\tilde{T}_g$ goes to zero as r increases. On the other hand, in $\tilde{T}_s$ only I_n appears since $\tilde{T}_s$ must be finite at $r=0$. A_n and B_n are constants to be determined to satisfy the boundary conditions, i.e., temperature and heat flux continuity at the filament surface

$$\tilde{T}_g(r=a)=\tilde{T}_s(r=a), \tag{7a}$$

$$K_s\left.\frac{\partial \tilde{T}_s}{\partial r}\right|_{r=a}-K_g\left.\frac{\partial \tilde{T}_g}{\partial r}\right|_{r=a}+h\tilde{T}_s(r=a)=\begin{cases}\sqrt{\frac{2}{\pi}}\frac{P_o}{2b}e^{-2z^2/b^2}\sin\phi & \text{for } \phi\in[0,\pi]\\ 0 & \text{for } \phi\in[\pi,2\pi]\end{cases}, \tag{7b}$$

where K is thermal conductivity and h is the heat transfer coefficient which accounts for heat losses by convection and radiation. The last term in Eq. (7b) is the intensity distribution of the linear Gaussian laser beam at the filament surface. By substituting Eqs. (6) into Eqs. (7) the constants A_n and B_n are determined and the filament and gas temperatures are obtained

$$\tilde{T}_g(r,z,\phi)=\int_{-\infty}^{\infty}e^{i\lambda z}\frac{P_o}{4\pi K_s\delta_s}\left[\sum_{n=-\infty}^{\infty}\frac{\frac{(-i)^n\cos(n\pi/2)}{\pi(1-n^2)}e^{-\lambda^2b^2/8}I_n(\delta_s a)}{K_n(\delta_g a)I_n'(\delta_s a)-GK_n'(\delta_g a)I_n(\delta_s a)+HK_n(\delta_g a)I_n(\delta_s a)}K_n(\delta_g r)e^{in\phi}\right]d\lambda, \tag{8a}$$

$$\tilde{T}_s(r,z,\phi)=\int_{-\infty}^{\infty}e^{i\lambda z}\frac{P_o}{4\pi K_s\delta_s}\left[\sum_{n=-\infty}^{\infty}\frac{\frac{(-i)^n\cos(n\pi/2)}{\pi(1-n^2)}e^{-\lambda^2b^2/8}K_n(\delta_g a)}{K_n(\delta_g a)I_n'(\delta_s a)-GK_n'(\delta_g a)I_n(\delta_s a)+HK_n(\delta_g a)I_n(\delta_s a)}I_n(\delta_s r)e^{in\phi}\right]d\lambda, \tag{8b}$$

where $H=h/K_s\delta_s$, $G=K_g\delta_g/K_s\delta_s$, and I_n' and K_n' are the derivatives of I_n and K_n, respectively. To obtain Eqs. (8) we have used the Fourier transform of the intensity distribution of the illumination $((P_o/4\pi)e^{-\lambda^2b^2/8})$ together with the Fourier expansion of the function

$$f(\phi)=\left\{\begin{matrix}\sin\phi & \text{for } \phi\in[0,\pi]\\ 0 & \text{for } \phi\in[\pi,2\pi]\end{matrix}\right\}=\sum_{n=-\infty}^{\infty}\frac{(-i)^n\cos(n\pi/2)}{\pi(1-n^2)}e^{in\phi}.$$

At the surface of the filament $(r=a)$ the temperature reduces to

$$\tilde{T}_s(a,z,\phi)=\int_{-\infty}^{\infty}e^{i\lambda z}\frac{P_oe^{-\lambda^2b^2/8}}{4\pi K_s\delta_s}\left(\sum_{n=-\infty}^{\infty}\frac{\frac{(-i)^n\cos(n\pi/2)}{\pi(1-n^2)}}{\frac{I_n'(\delta_s a)}{I_n(\delta_s a)}-G\frac{K_n'(\delta_g a)}{K_n(\delta_g a)}+H}e^{in\phi}\right)d\lambda. \tag{9}$$

When the filament radius is much smaller than the thermal diffusion length $(\mu=\sqrt{D/\pi f})$ only the term $n=0$ contributes to the temperature. Moreover, using the limiting forms of the Bessel functions for small arguments (see Eqs. 9.6.7 to 9.6.9 in Ref. 11), the following approximations hold: $I_o(z)\approx 1$, $I_o'(z)\approx z/2$, $K_o(z)\approx -Ln(z)$, and $K_o'(z)\approx -1/z$. Accordingly, the surface temperature for *thermally thin filaments*, which are the most interesting ones from a practical point of view, does not depend on ϕ, and writes

$$\begin{aligned}\tilde{T}_s(a,z)&\approx\int_{-\infty}^{\infty}e^{i\lambda z}\frac{P_o}{4\pi^2K_s\delta_s}\frac{e^{-\lambda^2b^2/8}}{\frac{I_o'(\delta_s a)}{I_o(\delta_s a)}-G\frac{K_o'(\delta_g a)}{K_o(\delta_g a)}+H}d\lambda\\&\approx\int_{-\infty}^{\infty}e^{i\lambda z}\frac{P_o}{4\pi^2K_s\delta_s}\frac{e^{-\lambda^2b^2/8}}{\frac{\delta_s a}{2}-G\frac{1}{\delta_g aLn(\delta_g a)}+H}d\lambda.\end{aligned} \tag{10}$$

Analytical solutions of Eq. (10) are found for two special cases

(a) In the absence of heat losses $(G=H=0)$ and using a tightly focused laser beam $(b\to 0)$ the temperature at surface of the thin filament is given by

$$\tilde{T}_s(a,z)\approx\frac{P_o}{2\pi K_sq_sa}e^{-q_s|z|}, \tag{11}$$

which represents a plane thermal wave propagating along the z axis. Under these conditions, both the natural logarithm of the amplitude, $Ln(\tilde{T})$, and the phase, ψ, of the surface temperature are parallel straight lines when represented as a function of z, with a slope $m_\Psi=m_{Ln(\tilde{T})}=-(\pi f/D_s)^{0.5}$.

(b) If heat conduction to the gas is neglected $(G=0)$ and using a tightly focused laser beam $(b\to 0)$ the temperature at surface of the thin filament is given by

$$\tilde{T}_s(a,z)\approx\frac{P_o}{2\pi K_sq_s'a}e^{-q_s'|z|}, \tag{12}$$

where $q_s'^2=q_s^2+(2h/K_sa)$. This result is similar to that found for thin slabs[6] and filaments.[12] According to Eq. (12), $Ln(\tilde{T})$ and Ψ are linear functions of z, but with different slopes. However, their product satisfies $m_\Psi\times m_{Ln(\tilde{T})}=-\pi f/D_s$, which is the generalization of the slope method.

To evaluate the effect of heat losses by conduction to the surrounding gas Eq. (10) must be used, since there is no simple analytical expression.

B. Two-layer cylinder

In the case of a coated cylinder with an inner layer of radius a_1 and an outer layer of radius a_2 [see Fig. 1(c)] surrounded by gas, the oscillating temperature in each layer and in the surrounding gas can be written as

$$\tilde{T}_g(r,z,\phi)=\int_{-\infty}^{\infty}e^{i\lambda z}\left[\sum_{n=-\infty}^{\infty}A_nK_n(\delta_g r)e^{in\phi}\right]d\lambda, \tag{13a}$$

$$\tilde{T}_2(r,z,\phi)=\int_{-\infty}^{\infty}e^{i\lambda z}\left[\sum_{n=-\infty}^{\infty}B_nI_n(\delta_2 r)e^{in\phi}+\sum_{n=-\infty}^{\infty}C_nK_n(\delta_2 r)e^{in\phi}\right]d\lambda, \tag{13b}$$

$$\tilde{T}_1(r,z,\phi)=\int_{-\infty}^{\infty}e^{i\lambda z}\left[\sum_{n=-\infty}^{\infty}D_nI_n(\delta_1 r)e^{in\phi}\right]d\lambda. \tag{13c}$$

Here subscripts 1 and 2 refer to layers 1 and 2, respectively. Note that in $\tilde{T}_2$ both K_n and I_n must be included. Constants A_n, B_n, C_n, and D_n are determined from the following boundary conditions

$$\tilde{T}_g(r=a_2)=\tilde{T}_2(r=a_2), \tag{14a}$$

$$\tilde{T}_1(r=a_1)=\tilde{T}_2(r=a_1), \tag{14b}$$

$$K_2 \left.\frac{\partial \tilde{T}_2}{\partial r}\right|_{r=a_1} = K_1 \left.\frac{\partial \tilde{T}_1}{\partial r}\right|_{r=a_1}, \tag{14c}$$

$$K_2 \left.\frac{\partial \tilde{T}_2}{\partial r}\right|_{r=a_2} - K_g \left.\frac{\partial \tilde{T}_g}{\partial r}\right|_{r=a_2} + h\tilde{T}_2(r=a_2) = \begin{cases} \sqrt{\frac{2}{\pi}}\frac{P_o}{2b_2}e^{-2z^2/b^2}\sin\phi & \text{for } \phi\in[0,\pi] \\ 0 & \text{for } \phi\in[\pi,2\pi] \end{cases}. \tag{14d}$$

An analytical solution can be found for the surface temperature of the coated cylinder under the following assumptions: (a) the cylinder is thermally thin, (b) the conduction to the air is neglected ($G=0$), and (c) the laser beam is tightly focused ($b\to 0$)

$$\tilde{T}_2(a_2,z)\approx \frac{P_o}{2\pi K_\parallel q'_\parallel a_2}e^{-q'_\parallel|z|}, \tag{15}$$

where $q'^2_\parallel=(i\omega/D_\parallel)+(2h/K_\parallel a_2)$, $K_\parallel=K_1v_1+K_2v_2$, $D_\parallel=K_\parallel/(\rho c)_{eff}$, and $(\rho c)_{eff}=(K_1/D_1)v_1+(K_2/D_2)v_2$. Here $v_1=(a_1^2/a_2^2)$ and $v_2=(a_2^2-a_1^2)/a_2^2$ are the volume fraction of layers 1 and 2, respectively.

By comparing Eq. (15) with Eq. (12) it can be concluded that the two-layer filament behaves as a monofilament with effective thermal conductivity ($K_\parallel$) and thermal diffusivity ($D_\parallel$), which follow the in-parallel thermal resistor model.[13]

In the particular case of a thin tube the inner core is empty, i.e., $K_1=0$, and Eq. (15) reduces to

$$\tilde{T}_2(a_2,z)\approx \frac{P_o}{2\pi K_2 q'_2 a'}e^{-q'_2|z|}, \tag{16}$$

where $q'^2_2=(i\omega/D_2)+(2h/K_2a')$ and $a'=(a_2^2-a_1^2)/a_2$. By comparing this expression with Eq. (12) it can be stated that the surface temperature of a thin tube behaves as of that a solid one of the same thermal properties but with an equivalent radius a'.

III. NUMERICAL CALCULATIONS

We focus our interest on poor thermal conductive filaments since their thermal diffusivity is more difficult to measure accurately, as explained in the introduction. According to Eq. (10) we have simulated the lateral dependence of $Ln(\tilde{T})$ and ψ for a polymeric monofilament of 60 μm of diameter. Its thermal properties are $D_s=0.15$ mm^2/s and $K_s=0.2$ Wm^{-1} K^{-1}, while the thermal properties of the surrounding air are $D_g=22$ mm^2/s and $K_g=0.026$ Wm^{-1} K^{-1}. Calculations have been performed with realistic experimental data: an exciting beam radius of $b=50$ μm, and a low modulation frequency of $f=0.1$ Hz, in order to avoid the influence of diffraction of the IR radiation. The continuous lines in Fig. 2 show the lateral behavior of $Ln(\tilde{T})$ and ψ in the absence of heat losses ($G=H=0$). As can be seen, far away from the heating spot, both are parallel straight lines from whose slope m the thermal diffusivity can be obtained $m_\psi=m_{Ln(T)}=-(\pi f/D_s)^{0.5}$, in agreement with Eq. (11). The dashed lines in Fig. 2 are the simulations for the filament kept in vacuum ($G=0$). In these conditions, only heat losses by radiation take place. Simulations have been performed with $h_{rad}=6$ Wm^{-2} K^{-1}, which is the highest value of h at room temperature, according to the Stefan–Boltzmann law.[9] In this case, the parallelism between $Ln(\tilde{T})$ and ψ has disappeared but there is a compensation of the slopes, in such a way that their product satisfies $m_\psi \times m_{Ln(\tilde{T})}=-\pi f/D_s$, in agreement with Eq. (12), indicating that the thermal diffusivity of the filament can be obtained in an easy way using the slope method. Finally, the dotted lines in Fig. 2 correspond to the filament surrounded by air. In these conditions, the three heat loss mechanisms are present. Simulations have been performed with $h_{rad+conv}=25$ Wm^{-2} K^{-1}, an appropriate value for vertical and slender filaments.[9,14] Anyway, it is worth mentioning that a h change in the range 10–50 Wm^{-2} K^{-1}, slightly affects the surface temperature. As can be seen, with the filament in air the linearity of both $Ln(\tilde{T})$ and ψ is drastically lost.

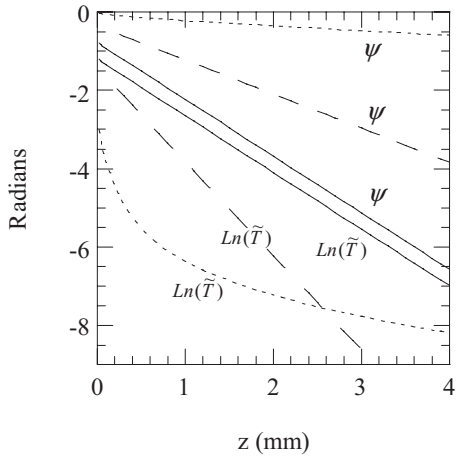

FIG. 2. Simulations of the lateral dependence of $Ln(\tilde{T})$ and ψ of a polymeric monofilament of 60 μm of diameter according to Eq. (10). Continuous lines: Absence of heat losses ($G=H=0$). Dashed lines: The filament is kept in vacuum ($G=0$). Dotted lines: The filament is surrounded by air. Data: $D_s=0.15$ mm^2/s, $K_s=0.2$ Wm^{-1} K^{-1}, $D_g=22$ mm^2/s, $K_g=0.026$ Wm^{-1} K^{-1}, $b=50$ μm, and $f=0.1$ Hz.

Summarizing we can conclude that heat loss by conduction to the surrounding gas is the most disturbing mechanism preventing from using the slope method to retrieve the thermal diffusivity of thin filaments. However, by keeping the filament in vacuum the slope method can be used accurately.

IV. EXPERIMENTAL RESULTS AND DISCUSSION

In order to verify the last conclusion we have used a lock-in thermography setup to measure the temperature profile of thin filaments heated by a focused and modulated laser beam. Filaments with very different diffusivity values, from polymers to metals, have been studied. Measurements have been performed at room temperature with the sample surrounded by air and with the sample enclosed in a vacuum chamber. An acousto-optically modulated laser beam (CO-

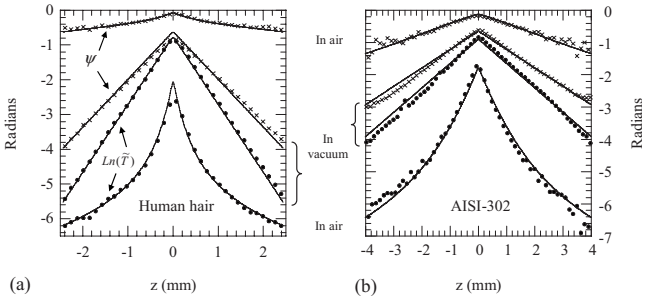

FIG. 3. Experimental values of the natural logarithm of the amplitude (dots) and phase (crosses) of the surface temperature of two monofilaments: (a) a human hair of 60 μm of diameter measured at $f=0.12$ Hz and (b) a stainless steel (AISI-302) wire of 25 μm of diameter measured at $f=0.48$ Hz. Measurements were performed in air and in vacuum. The solid lines are the best fittings of the data according to Eq. (10) with $b=50$ μm, $h=25$, $D_{\text{hair}}=0.14$ mm^2/s, and $D_{\text{AISI-302}}=3.6$ mm^2/s.

HERENT, model Verdi, $\lambda=532$ nm) focused onto the sample surface by a cylindrical lens of 10 cm focal length has been used to heat the filament. The IR radiation from the sample surface is captured by an IR camera (CEDIP, model JADE J550M, 3.6–5.0 μm) provided with a lens of 50 mm focal length. This lens has a minimum working distance of 23.5 cm, which gives a spatial resolution of 137 μm, i.e., each pixel measures the average temperature over a square on the sample of 137 μm in side. The lock-in software provided with the camera gives the amplitude and phase of the oscillating temperature. To improve the signal to noise ratio we record 4000 images for each experiment. As the noise level is inversely proportional to the square root of the total number of images (see p. 32 in Ref. 1), we obtain a temperature noise level as low as 1 mK. Measurements were carried out by heating one hemicylinder of the filament and recording the IR emission from the other hemicylinder. A silicon window placed in front of the camera lens was used to prevent the laser beam from reaching the camera lens.

To increase at the same time the absorption to the exciting light and the IR emissivity, some filaments (metals, transparent polymers, etc.) were covered by a 100 nm thick graphite layer. However, the obtained thermal diffusivity was the same as without the graphite layer in all cases. More relevant is the effect of the light reflected between the filament and the focusing lens which acts as a second heating source, illuminating almost uniformly the whole length of the filament.[15] The effect of this parasitic (modulated) light is to rise the wings of both amplitude and phase of the surface temperature, leading to an overestimation of the thermal diffusivity. To overcome this issue we have painted a small black dot on the filament in order to reduce the reflected light.

Figure 3 shows the experimental values of the natural logarithm of the amplitude (dots) and phase (crosses) of the surface temperature of two monofilaments: (a) a human hair of 60 μm of diameter measured at $f=0.12$ Hz and (b) a stainless steel (AISI-302) wire of 25 μm of diameter measured at $f=0.48$ Hz. Measurements were performed in air and in vacuum. Regarding the measurements performed in vacuum $Ln(\tilde{T})$ and ψ are not parallel as predicted by the theory, due to heat losses by radiation. By using the product of their slopes the thermal diffusivity of each filament is obtained: $D_{\text{hair}}=0.14$ mm^2/s and $D_{\text{AISI-302}}=3.6$ mm^2/s. Regarding the measurements performed in air the linearity of both $Ln(\tilde{T})$ and ψ is lost and, therefore, the slope method cannot be applied to retrieve the thermal diffusivity of the filaments, even in the case of the alloy wire. The continuous lines are the calculated values of the amplitude and phase of the surface temperature using Eq. (10) with $b=50$ μm. The agreement between experiments and simulations is excellent indicating the validity of the predictions of the theoretical model. In Table I, we summarize our measurements of the thermal diffusivity of several filaments using the slope method, with the sample kept in vacuum. The agreement with the literature values is very good, except in the case of polyether-ether-ketone (PEEK) fibers. As the retrieved value is independent of the fiber diameter the discrepancy is not due to heat losses. We think, instead, that this high value of the thermal diffusivity is related to the 45% crystallinity degree of these fibers, that has been demonstrated to enhance the thermal diffusivity of polymers.[19,20]

TABLE I. Thermal diffusivity of filaments. Measurements performed in vacuum. The uncertainty is 5%.

Material	Diameter (μm)	D (this work) (mm^2/s)	D (literature[a]) (mm^2/s)
Cu	50	120	116
Ni	125	19	22
Ti	125	8.8	9.0
AISI-302	125	3.8	3.7–4.0
AISI-302	25	3.6	3.7–4.0
AISI-302	10	3.6	3.7–4.0
Carbon fiber T650/35	7	6.4	8.8
Carbon fiber P100	10	310	325
PEEK	150	0.54	0.19
PEEK	34	0.52	0.19
Human hair	60	0.14	···

[a]References 16–18.

To verify the ability of the slope method to retrieve the effective thermal diffusivity of tubes and coated filaments we have taken data on a commercial hypodermic needle with an outer diameter of 0.414 mm and an inner diameter of 0.256 mm. We obtained a thermal diffusivity of 3.5 mm^2/s, a typical value of stainless steel. Then we covered some needles with different thicknesses of commercially available spray paint (matt black), in order to obtain increasing volume fractions of the coating layer: 0.14, 0.24, 0.46, 0.63, and 0.83. The results of the effective thermal diffusivity with the samples kept in vacuum are shown by dots in Fig. 4. The continuous line is the theoretical value of the in-parallel thermal resistor model, using $D_{\text{needle}}=3.5$ mm^2/s, $K_{\text{needle}}=15$ Wm^{-1} K^{-1}, $D_{\text{paint}}=0.2$ mm^2/s, and $K_{\text{paint}}=0.3$ Wm^{-1} K^{-1}, which are the typical values of spray paint. The agreement between the experimental values and the prediction supports the conclusion that the slope method can be used to measure the effective thermal diffusivity of coated filaments.

Lock-in thermography, as all transient experiments, are powerful tools to measure thermal diffusivity. However, they

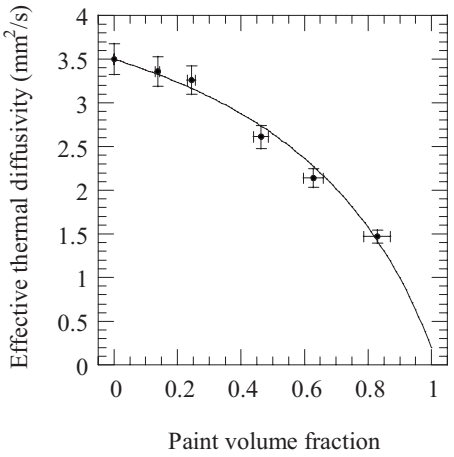

FIG. 4. Effective thermal diffusivity of a painted hypodermic needle as a function of the paint volume fraction. Dots are the experimental data and the continuous line is the calculated thermal diffusivity using the in-parallel thermal resistor model, using $D_{needle}=3.5$ mm^2/s, $K_{needle}=15$ Wm^{-1} K^{-1}, $D_{paint}=0.2$ mm^2/s, and $K_{paint}=0.3$ Wm^{-1} K^{-1}.

are unable to measure thermal conductivity, unless a reference is used. As a further application of the slope method, we have measured the effective thermal diffusivity of a hypodermic needle filled with water in order obtain the thermal conductivity of the needle. As a first steep, the thermal diffusivity of the empty needle was measured. Then, the effective thermal diffusivity of the needle filled with water was measured and the thermal conductivity of the needle was retrieved. Two hypodermic needles of different outer and inner radii were used: (a) $a_2=0.207$ and $a_1=0.105$ mm and (b) $a_2=0.157$ and $a_1=0.065$ mm. The lateral scans of $Ln(\tilde{T})$ and ψ for the thicker needle are shown in Fig. 5. The thermal diffusivity of both empty needles is the same, 3.6 mm^2/s, while the effective thermal diffusivities of the needles filled with water were 2.6 and 2.8 mm^2/s. By using the expression of the effective thermal diffusivity of a coated cylinder and using the thermal properties of water ($D_{water}=0.144$ mm^2/s and $K_{water}=0.60$ Wm^{-1} K^{-1}), the thermal conductivity of the needle was obtained: $K_{needle}=14$ Wm^{-1} K^{-1}, with an uncertainty of 10%. This value is close to the typical value of the thermal conductivity of stainless steel. On the other hand, it is worth noting that the uncertainty depends on the thickness of the tube wall. The thinner the wall the more accurate the retrieved thermal conductivity is.

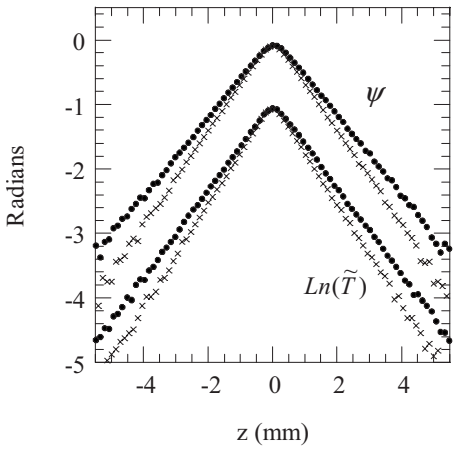

FIG. 5. Lateral dependence of $Ln(\tilde{T})$ and ψ for a hypodermic needle with an outer diameter of 0.414 mm and an inner diameter of 0.210 mm. Measurements were performed for an empty needle (dots) and for the needle filled with water (crosses).

V. SUMMARY AND CONCLUSIONS

In this work, we have calculated the surface temperature of both solid and coated filaments illuminated by a modulated and tightly focused laser beam. Heat losses by radiation, convection, and conduction to the surrounding gas have been taken into account. Calculations show that, as in thin plates, conduction to the surrounding gas is the mechanism responsible for the lost of linearity observed in the phase ψ and in the natural logarithm $Ln(\tilde{T})$ of the surface temperature when the sample is placed in air. The calculations also demonstrate that when suppressing the surrounding gas (only radiative heat losses are present), ψ and $Ln(\tilde{T})$ keep a linear behavior as a function of the distance to the heating spot. In this case, the slopes of ψ and $Ln(\tilde{T})$ are modified with respect to their values in the absence of heat losses, but their product only depends on the diffusivity of the material. Accordingly, we conclude that accurate measurements of the thermal diffusivity can be obtained by placing the samples in a vacuum chamber. Moreover, we have demonstrated analytically that the effective diffusivity of coated filaments agrees with the in-parallel thermal resistor model.

All these conclusions have been validated by performing lock-in thermography measurements at low frequencies in a wide set of single and coated filaments, as well as in hollow and filled thin tubes. From the data obtained by placing the samples in a vacuum chamber, we have obtained accurate values of the thermal diffusivity of filaments (from 0.14 mm^2/s in a human hair to 310 mm^2/s in a carbon fiber) of several diameters, some of them as thin as 7 μm of diameter. Moreover, the excellent agreement between the full calculations of the temperature and the experimental data taken in air confirm that the conduction to the air is the mechanism responsible for the bending of the surface temperature amplitude and phase. On the other hand, using stainless steel hypodermic needles covered with different thicknesses of black paint, we have experimentally confirmed that the effective thermal diffusivity of a coated filament behaves according to the in-parallel thermal resistor model. Finally, we have obtained the thermal conductivity of the uncoated needles by filling them with water.

ACKNOWLEDGMENTS

This work has been supported by the Ministerio de Educación y Ciencia (Grant No. MAT2008-01454).

[1] O. Breitenstein and M. Langenkamp, *Lock-in Thermography* (Springer, Berlin, 2003).
[2] The linearity behaves for $Ln(r^n\tilde{T})$ where $n=0$, 0.5, and 1 for 1D, 2D, and 3D heat propagation, respectively.
[3] L. Fabbri and P. Fenici, Rev. Sci. Instrum. **66**, 3593 (1995).
[4] B. Zhang and R. E. Imhof, Appl. Phys. A: Mater. Sci. Process. **62**, 323 (1996).
[5] J. F. Bisson and D. Fournier, J. Appl. Phys. **83**, 1036 (1998).

[6]A. Wolf, P. Pohl, and R. Brendel, J. Appl. Phys. **96**, 6306 (2004).
[7]J. Hou, X. Wang, and J. Guo, J. Phys. D **39**, 3362 (2006).
[8]A. Mendioroz, R. Fuente, E. Apiñaniz, and A. Salazar, Rev. Sci. Instrum. **80**, 074904 (2009).
[9]A. Salazar, A. Mendioroz, and R. Fuente, Appl. Phys. Lett. **95**, 121905 (2009).
[10]J. H. Barkyoumb and D. J. Land, J. Appl. Phys. **78**, 905 (1995).
[11]*Handbook of Mathematical Functions*, edited by M. Abramowitz and I. A. Stegun (Dover, New York, 1965).
[12]C. Pradère, J. M. Goyhénèche, J. C. Batsale, S. Dilhaire, and R. Pailler, Int. J. Therm. Sci. **45**, 443 (2006).
[13]J. E. Parrot and A. D. Stukes, *Thermal Conductivity in Solids* (Pion, London, 1975), p. 129.
[14]T. Cebeci, Proceedings of the Fifth International Heat Transfer Conference, publication NCI.4, 15 (1974).
[15]D. Fournier, W. Coatesworth, and J. P. Roger, Anal. Sci. **17**, s490 (2001).
[16]http://www.goodfellow.com
[17]H. Kato, T. Baba, and M. Okaji, Meas. Sci. Technol. **12**, 2074 (2001).
[18]L. R. Touloukian, R. W. Powell, C. Y. Ho, and M. C. Nicolasu, *Thermal Diffusivity* (IFI/Plenum, New York, 1973).
[19]C. L. Choy, G. W. Yang, and Y. W. Wong, J. Polym. Sci., Part B: Polym. Phys. **35**, 1621 (1997).
[20]C. L. Choy, Y. W. Wong, G. W. Yang, and T. Kanamoto, J. Polym. Sci., Part B: Polym. Phys. **37**, 3359 (1999).